EUROFUSION WP14ER-PR(15) 14675

F Consoli et al.

Time-resolved absolute measurements by electro-optic effect of giant electromagnetic pulses due to laser-plasma interaction in nanosecond regime

Preprint of Paper to be submitted for publication in Physical Review Letters

This work has been carried out within the framework of the EUROfusion Consortium and has received funding from the Euratom research and training programme 2014-2018 under grant agreement No 633053. The views and opinions expressed herein do not necessarily reflect those of the European Commission.

Time-resolved absolute measurements by electro-optic effect of giant electromagnetic pulses due to laser-plasma interaction in nanosecond regime

F. Consoli[a] , R. De Angelis[a], L. Duvillaret[b], P.L. Andreoli[a], M. Cipriani[a], G. Cristofari[a], G. Di Giorgio[a], F. Ingenito[a]

[a]*ENEA for EUROfusion, Via E. Fermi 45, 00044 Frascati, Italy*

[b]*Kapteos, Alpespace - bât. Cleanspace 354 voie Magellan, 73800 Sainte-Hélène du Lac, France*

Corresponding author: F. Consoli, ENEA - Centro Ricerche Frascati, FSN-FUSPHY-SAD, Via E. Fermi 45, 00044 Frascati (Rome), Italy, email: fabrizio.consoli@enea.it, tel: +390694005415

Abstract

We describe the first absolute measurements of electromagnetic pulses (EMPs) generated by laser-plasma interaction in nanosecond regime, with laser intensities typical for inertial-confinement-fusion, by means of the electro-optic effect on dielectric crystals. This allowed us to perform the first direct measurement with the detector rather close and in direct view of the plasma. A maximum field of 260.9 kV/m was measured, orders of magnitude higher than measurements by conductive probes on nanosecond regime lasers with much higher energy. The analysis of measurements and of particle-in-cell simulations indicates that signals match the emission of charged particles detected in the same experiment, and suggests that anisotropic particle emission from target, X-ray photoionization and charge implantation on surfaces directly exposed to plasma, could be important EMP contributions.

The interaction of high energy and high intensity lasers with matter produces particle and electromagnetic radiation over wide ranges [1,2]. The generation of transient fields of very high intensity in the radiofrequency-microwave regime has been observed for femtosecond to nanosecond laser pulses with 10^{11}-10^{20} W/cm^2 intensity, on conductive and dielectric targets [3-21]. These fields can have several gigahertz bandwidths and last for hundreds of nanoseconds. They can induce blindness and often damages in electronic equipment inside and near the experimental chamber. On the other hand, once the sources are well understood they might be also used as effective diagnostic tool.

The absolute characterization of these electromagnetic pulses (EMPs) is for these reasons of primary importance and nowadays a very hot topic for existent and future plants for laser-plasma acceleration (*PETAL* [22], *ELI* [23,24],…) and for inertial-confinement-fusion (*NIF* [6,12,13], *LMJ* [21],…).

EMPs have been commonly characterized by means of conductive probes [3-21], but only a few works deal specifically with absolute measurements of the associated electric fields, which are accomplished by D-dot and B-dot probes (sensitive to $\dot{D}$ and $\dot{B}$ respectively) [25,26]. This also for the difficulty of performing reliable measurements with suitable signal-to-noise ratio (SNR). The conductive structure of these probes usually determines low measurement accuracy in near field characterization [27]. This is a serious problem in experimental chambers for laser-plasma-interaction (LPI) experiments, commonly crowded of metallic equipment, and sets a limit on the probe minimum distance from the interaction locus. These probes cannot be put in direct view of the plasma because parasitic currents can be induced on them by ionizing radiation emitted from plasma (charged particles, and UVs-Xrays by photoelectric effect), and can propagate to the oscilloscope heavily affecting the E-field measurement. EMPs may further induce spurious currents on the external conductor of the coaxial cables connecting the probes to the oscilloscope. Moreover, time integration is required to get electric fields from $\dot{D}$ measurements; this greatly amplifies the low-frequency noise (where important part of the signal is), and requires suitable filtering [6]. $\dot{B}$ measurements are even worst, since plane-wave approximation (inappropriate inside a conductive chamber) is used. In this work we describe the first (to the author's knowledge) time-resolved direct measurements, using the linear electro-optic (Pockels) effect in crystals [28], of single vectorial components of EMP electric fields due to laser-plasma interactions on nanosecond regime, at laser intensities typical of inertial-confinement-fusion (ICF). This allowed us to perform, for the first time, measurements with the detector in direct view of the plasma and rather close to it.

Dielectric electro-optic (EO) probes have allowed reliable measurement of transient electric fields [29-34], with important advantages on classical conductive probes, in terms of field vectorial selectivity (one component measurement rejecting the orthogonal ones), bandwidth, dynamics, temporal and spatial resolution, low dimensions and invasiveness [31-33,35,36]. Indeed, their effective permittivity may induce a local perturbation on fields measured in vacuum, but this remains much lower and localized than for conductive probes [31-33], and offline calibration permits proper estimation and de-embedding [31-33]. The fully dielectric structure insures no parasitic currents even in these harsh environments. Their intrinsic low sensitivity is generally not detrimental when dealing with high intensity field measurements, like for EMPs. So far, they have been used in air, water, and for atmospheric pressure plasma jet sources [31,33,37-39]. Here we document about their application in vacuum and specifically in LPI.

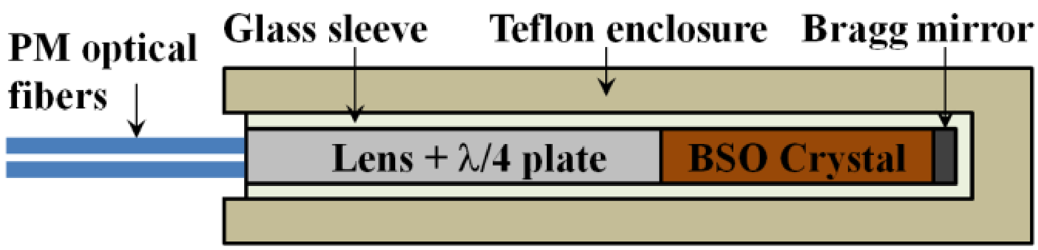

Figure 1. Scheme of the EO-probe.

A main scheme of the EO-probe structure is in Fig.1 [31,40]. Measurements of external electric fields are performed by detecting the change of polarization state, induced by the electro-optic effect, of a continuous-wave laser probing beam having λ = 1550 nm and circular polarization, propagating in a <111>-cut $\bar{4}3$ m $Bi_{12}SiO_{20}$ (BSO) crystal of 5 mm length. This is the *polarization state modulation* technique [29-33,41,42]. BSO is intrinsically isotropic, becoming here birefringent because of the $\vec{E}_\perp$ component of the external field, orthogonal to the laser wave-vector $\vec{k}$ placed parallel to the <111> direction of the crystal. Indeed in Fig.1 $\vec{k}$ is slightly misaligned with this direction, so to that light coming from the first fiber can be collected by the second, after total reflection on the dielectric Bragg mirror. Elliptical polarization on the output probe beam is caused by the generated anisotropy; information on electric field is contained on 1) induced dephasing between the two linearly-polarized components of the elliptical polarization: $\Delta\theta \propto |\vec{E}_\perp|$, and 2) orientation of eigendielectric axes with respect to the $< 11\bar{2} >$ optical axis: $\xi_\pm = \pi\,(3\pm1)/4 - \alpha_E/2$, being α_E the angle between $\vec{E}_\perp$ and the axis [30,41-42]. Thus, by using a wave polarization analyzer [41,42], the two components of $\vec{E}_\perp$ can be simultaneous measured with a single laser beam [29-33,41,42].

Kapteos^{TM} built a custom version of the EOP-P2R02-BS050 probe, expressly to adapt it to vacuum conditions used in the experimental chamber of ABC facility [43]. A polarization maintaining (PM) fiber is joined to the set of lens + λ/4 plate, followed by the crystal-mirror one (Fig.1). A glass sleeve (30 mm length and 4 mm diameter) contains the whole structure. The custom probe was then enclosed in a 3 mm thick Teflon shield, protecting it from direct X-ray radiation coming from the plasma. The shield permittivity ~2.1, leads to partial impedance matching of the probe (permittivity ε_{r}-

$_{eff}$ ~ 9 [30-33]) with the surrounding vacuum, increasing the sensitivity. The small bandwidth, around 1550 nm, of the detecting system (tailored infrared fast photodiodes, PM fibers and optics) allows effective rejection of possible coupling with the main laser (λ_0 = 1054 nm), and possible 400-700 nm light emission from scintillation of BSO by X-rays [44-46]. All constituents are dielectric and non-magnetic, with ultra-low loss tangent; the probe is insensitive to magnetic fields up to more than 3 T [35], three orders higher than those expected in this experiment. The full optical link allowed the electronics to be placed suitably far from experiment, eliminating their free-space-coupling with EMP. The EO effect occurs on femtosecond time-scales, leading to intrinsic bandwidths exceeding 10 THz, with f_{min} in the kilohertz range [31]. Indeed, here the system f_{max} was ~9 GHz, due to photodiode frequency cutoffs and round-trip time of laser through the crystal. The sensitivity of complete setup was preserved by using two tailored vacuum optical-feedthroughs with minimum insertion loss. The eoSense HF-2A-09L instrument provided laser probe generation, monitored probe sensitivity along time, executed demodulation and determination of the $E_{X'}$ and $E_{Y'}$ components of $\vec{E}_{\perp}$. To improve the SNR, dedicated low-noise-amplifiers were employed before of the 3.5 GHz Lecroy-735Zi oscilloscope. Offline calibrations of the probe setup by a TEM cell provided precise data on orientation of the crystal axes, measurement dynamics (> 120 dB Hz$^{0.5}$), intrinsic sensitivity (< 20 kV/m for single shot pulses), vectorial selectivity (> 40 dB) and spatial resolution (< 5 mm), whereas the field sign was still undetermined. The system is intrinsically robust to temperature variations and its stability was verified during the campaign.

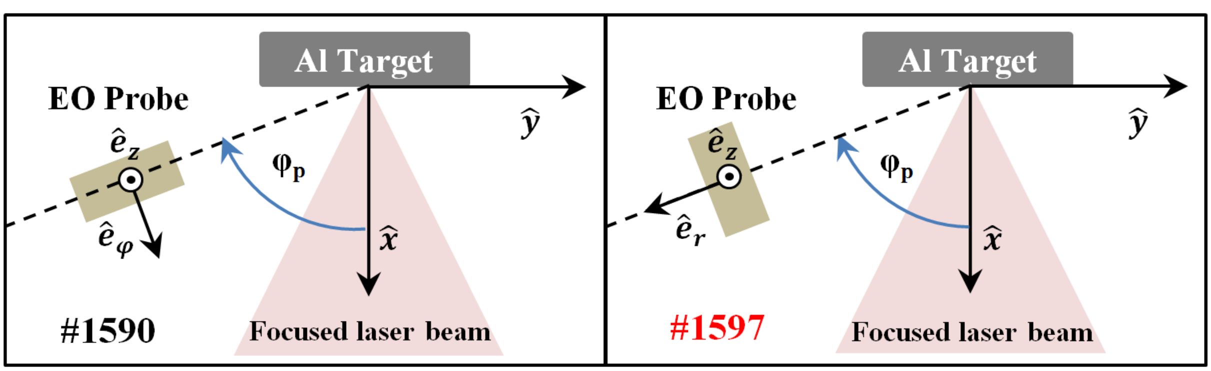

Figure 2. Scheme of the experiment in the two configurations represented by the shots #1590 and #1597.

Experiments have been performed with ABC laser, a Nd:phosphate-glass nanosecond facility [43]. One circularly polarized beam of 20-30 J, with FWHM ~ 3 ns, fundamental wavelength λ_0 and 10^{-5} contrast, was focused by a F/1 lens up to 50 μm diameter, leading to ~(0.3-0.5) PW/cm^2 intensity, for normal incidence on a thick (1710-1790 mm) Al target (Fig.2). For each shot the LPI was monitored by a considerable number of diagnostics [43]. Thermal ion emission from plasma was inspected by Time-of-Flight (TOF) detection with a set of faraday-cups; a particle contribution with E_{ion}/A ~ 1 keV (A= atomic number) is shown in Fig.3a at $\varphi = 53^o$ from the target normal. As evident, strong coupling with EMP oscillations hides detection of particles with energy ≥ 4 keV. The problem is overcome with TOF monocrystalline diamond detectors [47,48], fabricated by University of Tor Vergata with microstrip surface-interdigital connections and high hardness to EMPs [49]. In Fig.3b signal measured by a diamond placed at $\varphi = 65^o$ is shown in the electron-energy domain. The huge peak on the right is due to X-rays; on its left falling edge a clear indication of fast electrons is present, with 26 keV peak energy and 40% FWHM. Part of this hot electron population is due to resonant absorption [1,50,51], because of highly focused intensity (even higher in some regions because of self-focusing), large focusing angle (F/1 lens) and laser circular polarization. Part of this population is instead due to the two-plasmon-decay instability [1,50,52], also generating the $2\lambda_0/3$ = 703 nm harmonics [50,52]. In Fig.3d the visible light spectrum detected by the Ocean Optics HR4000 spectrometer is shown, with the clear indication of components at λ_0, $2\lambda_0/3$, and $\lambda_0/2$ (527 nm). Hot electrons escaping from plasma create an electrostatic Debye sheath which tugs the ions, accelerated by the potential drop [2]. On the same diamond signal the trace of ~20 keV fast protons (always present on any target surface as impurity [2]) was in fact detected (Fig.3c), together with the 1 keV thermal peak measured by the faraday-cup.

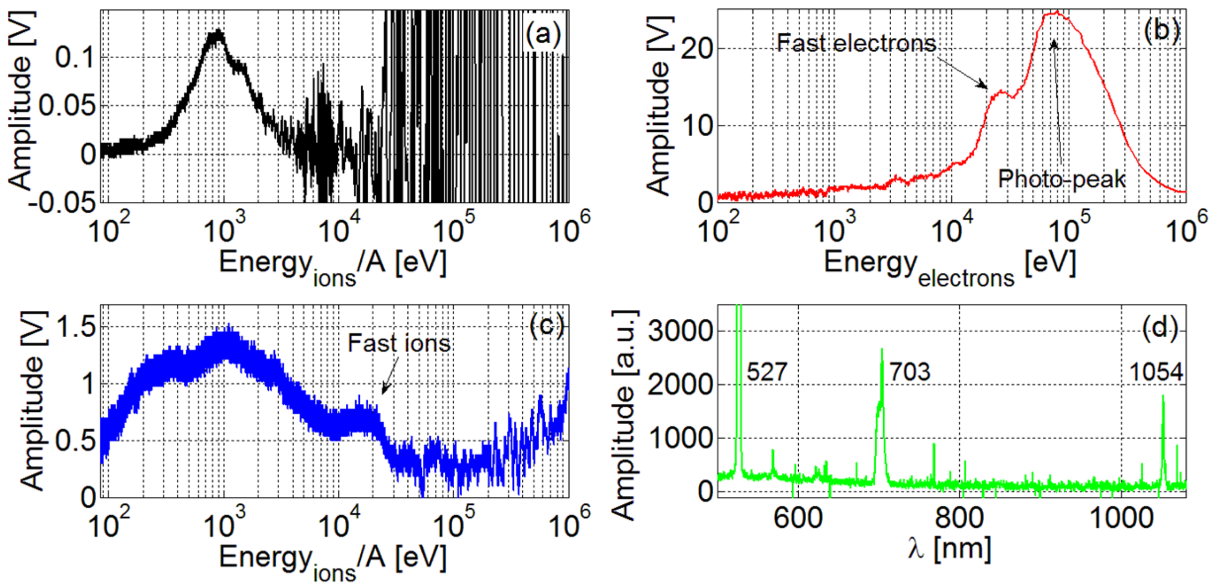

Figure 3. (a) Faraday-cup at 53°. Diamond detector at 65°: (b) electron and (c) ion energy domain. Optical spectrometer: detected light (d). A = atomic mass number.

We performed two series of measurements, with the EO-probe in direct view of the target and at 85 mm distance. For the first series the probe was mounted on the *xy* plane, as in configuration indicated for shot #1590 in Fig.2, with φ_p = 70°, longitudinal axis parallel to $\hat{e}_r$ in cylindrical coordinates and Bragg mirror toward the target. In the whole campaign we were able to measure the $\hat{e}_{1X'}$ component of $\vec{E}_\perp$, but not the $\hat{e}_{1Y'}$ one, because of technical reasons: lower sensitivity to this component and increased background noise of the associated channel amplifier. In particular, it was (Fig.2) $\hat{e}_{1X'} = \sin\gamma\,\hat{e}_\varphi + \cos\gamma\,\hat{e}_z \approx \hat{e}_\varphi + 0.16\,\hat{e}_z$, being γ = 81° ± 3°. In Fig.4a-b the measured $E_{1X'}$ component is shown for shot #1590 of this first series, in two different time scales; the axis origin was chosen at the beginning of the first intense peak. The signal appears to be constituted by two spectral components, as also shown in Fig.5. The main contribution lasts for the total signal duration (~1 μs) and concerns frequencies lower than ~50 MHz. The second affects only the first 300 ns and contains higher frequencies. Maxima higher than 100 kV/m are present in around the first 250 ns. Background noise is visible for t < 0, leading to very good SNRs for each shot. In the whole campaign it was not possible to determine the absolute field phase (i.e. sign). For this #1590 shot, a first high 'positive' peak is present (FWHM = 6.7 ns) and then a 'negative' large peak at ~40 ns. Thus, a rather sharp one is at ~80 ns, where the field reaches its maximum value: $\max|E_{1X'}|_{\#1590} = 216.5$ kV/m. From rough plane-wave approximation and on the hypothesis of isotropic emission with respect to target, the EMP energy is estimated ~0.46 J, ~1.8% of the laser one.

A superwideband (SWB) antenna was also used at ~48 cm from the target [14-16,53], in a region of the chamber well protected against direct plasma radiation by thick conductive objects. Results in time and frequency domain are compared in Fig.5 with those from EO-probe. The SWB signal duration is lower, whereas its main spectral contributions near ~130 MHz and ~200 MHz find correspondence in the EO signal. Since EO components for f < 50 MHz are instead missing, we could suppose these might be due to direct plasma radiation (X-rays and particles).

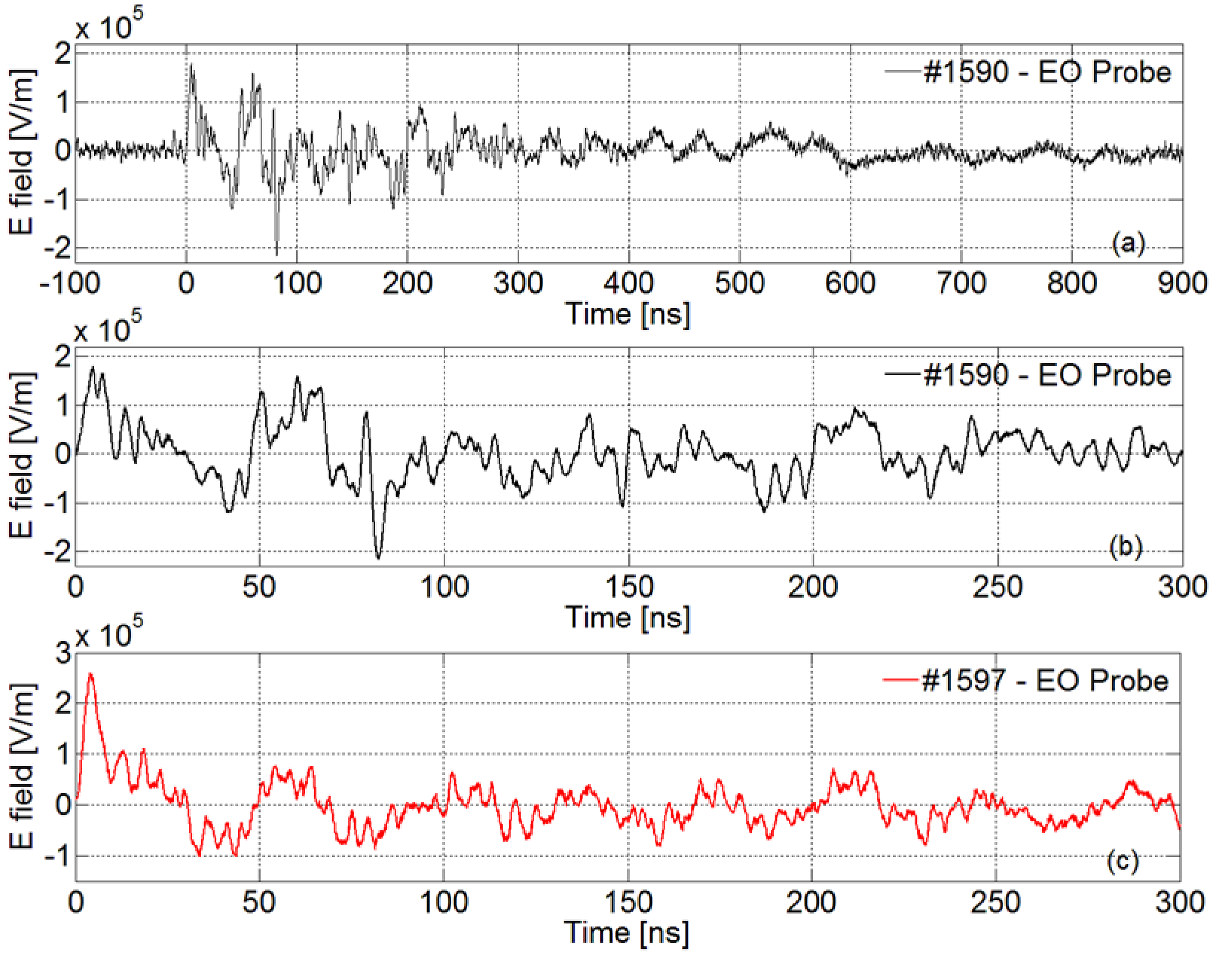

Figure 4. Measured $E_{X'}$ field component for shot #1590 (a and b, in two different time scales) and #1597 (c).

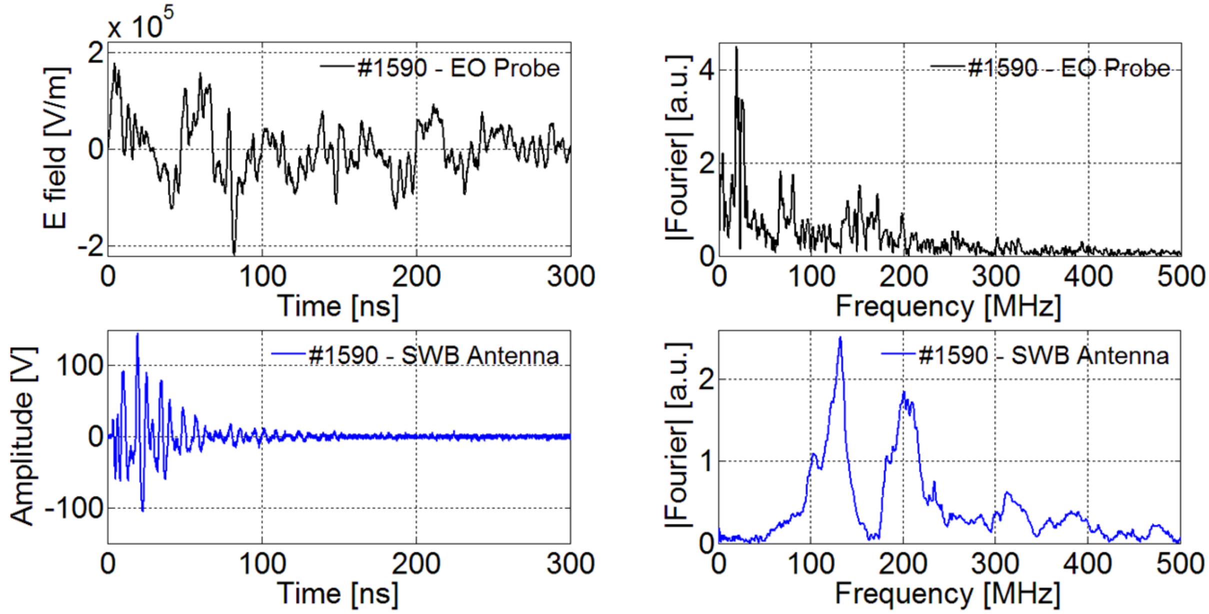

Figure 5. Time and frequency domain of signals of EO-probe and SWB antenna for shot #1590.

In the second series of measurements, probe was rotated of 90° clockwise with respect to the z axis (shot #1597 in Fig.2), so $\hat{e}_{2X'} \approx \hat{e}_r + 0.16\,\hat{e}_z$. In Fig.4c the related $E_{2X'}$ component is shown. Presence and time-duration of the two spectral contributions observed for shot #1590 are confirmed here, too. There is still a high sharp 'positive' peak (correspondent to that of shot #1590) having FWHM = 5.4 ns, leading to $\max|E_{2X'}|_{\#1597} = 260.9$ kV/m. Then, the field slowly decreases, changing sign at ~30 ns. There are some large oscillations, decreasing below 100 keV/m after ~80 ns from the main peak. The time evolution for t > 300 ns is similar to shot #1590, and then not reported. In this case the EMP energy is 0.54 J, ~2.2% of laser one.

To have better insight on possible origins of signals observed, we performed simplified particle-in-cell (PIC) simulations of the experiment, by CST Particle Studio solver. Space-charge effects were considered, together with secondary electron emission from teflon [54] and superficial charge deposition on surfaces. The target surface was source of conical particle flows, uniform within their angle of emission φ_t to the symmetry axis. We considered a Gaussian-shaped electron bunch with σ = 3 ns, 26 keV of peak energy, and 40% energy spread, as estimated from diamond measurements (Fig.3b). An equal and synchronized bunch of protons was added, modeling the fast ion component. In Fig.6a-6b, we compare EO-probe measurements with results of simulations for φ_t = 60°. The first peak on measured $E_{1X'}$ can be effectively associated with the simulated fast-electron peak, whereas simulated fast ions can be associated with the following measurement decrease, having minimum at ~40 ns. Later oscillations might be associated to quasi-neutral thermal components, not considered in these preliminary simple calculations. Future and more accurate modelings of the experiment have to consider photoionization due to the X-rays from plasma, generating a cloud of cold electrons around the external surface of the teflon. This is expected to originate a pulsed electric field, rather synchronous with the peak due to fast electrons. Effects due to charge implantation on teflon have to be taken carefully into account, too. These phenomena could help to explain why the first peak of measured $E_{2X'}$ is not present in these preliminary simulations, and the higher intensity of measured $E_{1X'}$ peak. On Figure 6c-6d we show simulations versus φ_t angle; when $\varphi_t > 70^o$ particles hit the probe. $E_{1X'}$ ($\sim E_\varphi$) decreases with φ_t and it is thus ascribable to anisotropic particle emission from target with respect to the probe. Indeed, E_φ became negligible in simulations with the EO-probe on the symmetry axis of the particle flow. On the other hand, $E_{2X'}$ ($\sim E_r$) is not particularly affected by this (Fig.6d).

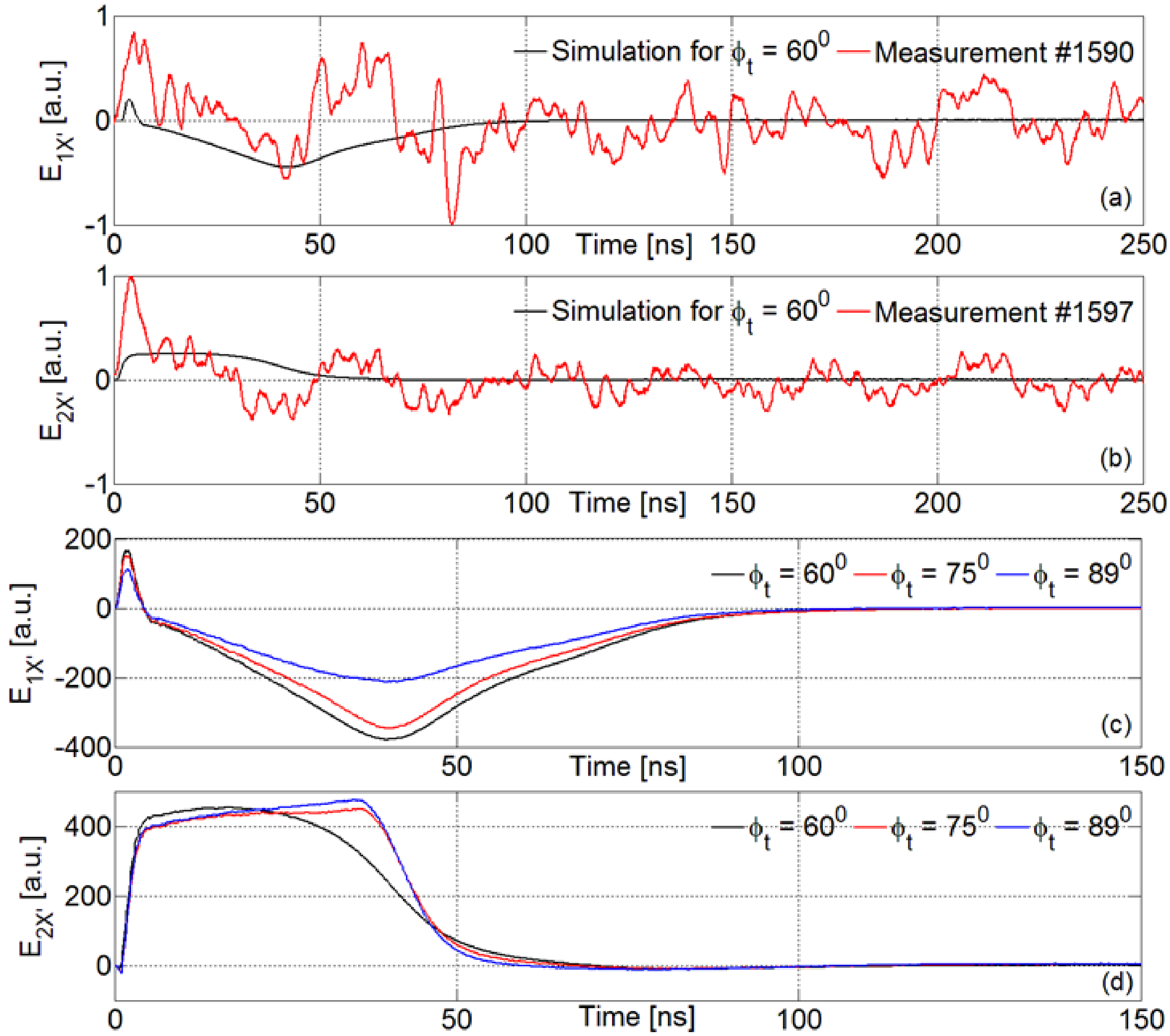

Figure 6. Measurement of a) $E_{1X'}$ in shot #1590 and b) $E_{2X'}$ in shot #1597, with related simulations for $\varphi_t = 60^o$; c) and d): simulations for $E_{1X'}$ and $E_{2X'}$ for different φ_t.

In summary, in this work we have shown the first direct measurements, by means of dielectric EO-probes directly viewing the plasma, of the electric field of EMPs generated by laser-target interaction in ICF regime. A maximum electric field of 260.9 kV/m was measured, more than an order of magnitude higher than previous measurements in nanosecond lasers with much higher energy (LULI, OMEGA and NIF [6,8,10,12,13,20,21]), and comparable with maximum values reached with picosecond lasers [20,21].

The analysis of measurements and of preliminary simulations indicates that achieved EMP signals are compatible with the emission of TOF-detected charged particles [10]. It also shows that EMP should be affected by anisotropic particle emission from target, X-ray photoionization and charge implantation on surfaces directly exposed to the plasma. In experiments with femtosecond laser of

~100 mJ (with rather moderate plasma ionizing-radiation) the main EMP contribution resulted from neutralization-currents in the target holder [18]. In nanosecond facilities high intensity neutralization-currents were measured [55], but their contribution to EMP should be strongly inhibited [18]. Fig.5 suggests that here this could be associated with the main spectral components ~130 MHz and ~200 MHz detected by the SWB antenna.

The performed measurements allowed to get important information on effects due to laser-plasma interaction. Future experiments of this type and tailored numerical studies will be important for the better understanding of EMP sources in different regimes, key point of future plants for laser-plasma acceleration and for inertial-confinement-fusion, as well as for the use of EMPs as powerful plasma diagnostics. Moreover, the demonstration that electro-optic effect can be such an efficient method for detecting electric fields in laser-plasma context, opens to new possibilities of characterization of the intrinsic interaction and of the generated terahertz radiation.

Acknowledgments

This work has been carried out within the framework of the EUROfusion Consortium and has received funding from the Euratom research and training programme 2014-2018 under grant agreement No 633053. The views and opinions expressed herein do not necessarily reflect those of the European Commission. We warmly acknowledge the help of J. Dahdah from Kapteos for the EO-probe calibrations, of C. Verona from University of Tor Vergata for CVD Diamond detectors, and of E. Di Palma from ENEA - Centro Ricerche Frascati for his advices on CST simulation solver.

References

[1] W.L. Kruer, *The Physics of Laser Plasma Interactions* (Westview Press, Oxford, 2003).

[2] P. Gibbon, *Short Pulse Laser Interactions with Matter* (Imperial College Press, London, 2005).

[3] J. S. Pearlman, and G. H. Dahbacka, J. Appl. Phys. **49,** 457 (1978).

[4] M. J. Mead, D. Neely, J. Gauoin, R. Heathcote, and P. Patel, Rev. Sci. Instrum. **75**, 4225 (2004).

[5] J.L. Remo, R.G. Adams, and M.C. Jones, Appl. Opt. **46,** 6166 (2007).

[6] D. C. Eder et al, Lawrence Livermore National Laboratory, Report LLNL-TR-411183, 2009.

[7] A. V. Kabashin, P. I. Nikitin, W. Marine, and M. Sentis, Appl. Phys. Lett. **73,** 25 (1998).

[8] J. Raimbourg, Rev. Sci. Instrum. **75**, 4234 (2004).

[9] H. Nakajima, Y. Shimada, T. Somekawa, M. Fujita, and K.A. Tanaka, IEEE Geosci. Remote Sens. Lett. **6**, 718 (2009).

[10] J. A. Miragliotta, B. Brawley, C. Sailor, J.B. Spicer, and J.W.M. Spicer, in Proceedings of Laser Radar Technology and Applications XVI, Orlando (Florida), April 2011, edited by M.D. Turner and G.W. Kamerman, Proceedings of SPIE vol. 8037, 80370N.

[11] N.L. Kugland, B. Aurand, C.G. Brown, C.G. Constantin, E.T. Everson, S.H. Glenzer, D.B. Schaeffer, A. Tauschwitz, and C. Niemann, Appl. Phys. Lett. **101,** 024102 (2012).

[12] C.G Brown Jr., A. Throop, D. Eder, and J. Kimbrough, J. Phys.: Conf. Ser. **112**, 032025 (2008).

[13] C. G. Brown Jr., E. Bond, T. Clancy, S. Dangi, D.C. Eder, W. Ferguson, J. Kimbrough, and A. Throop, J. Phys.: Conf. Ser. **244,** 032001 (2010).

[14] F. Consoli et al, Nucl. Instrum. Meth. A **720**, 149 (2013).

[15] F. Consoli, R. De Angelis, P. Andreoli, G. Cristofari, and G. Di Giorgio, Phys. Procedia **62**, 11 (2015).

[16] F. Consoli, R. De Angelis, P. Andreoli, M. Cipriani, G. Cristofari, G. Di Giorgio, and F. Ingenito, in Proceedings of the IEEE 15th International Conference on Environment and Electrical Engineering (EEEIC), Rome, June 2015, edited by L. Martirano, R. Araneo, Z. Leonowicz, M.C. Falvo, p.182.

[17] J.-L. Dubois et al, Phys. Rev. E **89**, 013102 (2014).

[18] A. Poyé et al, Phys. Rev. E **91**, 043106 (2015).

[19] J.J. Santos et al, New J. Phys. **17**, 083051 (2015).

[20] F. Lubrano-Lavaderci, J.-L. Dubois, J. Gazave, D. Raffestin, and S. Bazzoli, Chocs – Revue scientifique et technique de la Direction des applications militaires **44**, 34 (2013).

[21] A. Poyé et al, “ElectroMagnetic Pulses induced by high intensity laser”, PETA-phys&PETAL+ Workshop, Institut Mathématique de Bordeaux, 24 February 2015 (unpublished).

[22] A. Casner et al, High Energ. Dens. Phys. **17**, 2 (2015).

[23] G. Mourou, G. Korn, W. Sandner, and J.L. Collier, *ELI - Extreme Light Infrastructure: Science and Technology with Ultra-Intense Lasers, Whitebook* (THOSS Media GmbH, Berlin, 2011).

[24] B. Le Garrec, S. Sebban, D. Margarone, M. Precek, S. Weber, O. Klimo, G. Korn, and B. Rus, in Proceedings of High Energy/Average Power Lasers and Intense Beam Applications VII, San Francisco, February 2014, edited by S.J. Davis, M.C. Heaven, J.T. Schriempf, in Proceedings of SPIE 8962, 89620I.

[25] C.E. Baum, E.L. Breen, J.C. Giles, J. O'Neill, and G.D. Sower, IEEE Trans. Antennas Propag. **AP-26,** 22 (1978).

[26] W.R. Edgel, “Primer on electromagnetic field measurements, Prodyn Application note, PAN 895; “Electric and magnetic field sensor application”, Prodyn Application note, PAN 192.

[27] C.A. Balanis, *Antenna Theory: Analysis and Design* (Wiley-Interscience, Hoboken, 2005).

[28] A. Yariv, and P. Yeh, *Photonics – Optical Electronics in Modern Communications* (Oxford University Press, London, 2007).

[29] L. Duvillaret, S. Riallad, and J.-L. Coutaz, J. Opt. Soc. Amer. B. **19**, 11, 2692 (2002); **19**, 11, 2704 (2002);

[30] G. Gaborit, J.-L. Coutaz, and L. Duvillaret, Appl. Phys. Lett. **90**, 241118 (2007).

[31] G. Gaborit, J. Dahdah, F. Lecoche, P. Jarrige, Y. Gaeremynck, E. Duraz, and L. Duvillaret, IEEE Trans. Plasma Sci. **41,** 2851 (2013).

[32] G. Gaborit, P. Jarrige, Y. Gaeremynck, A. Warzecha, M. Bernier, J.-L. Lasserre, and L. Duvillaret, in Ultra-Wideband, Short-Pulse Electromagnetics, Vol.10, p. 411, edited by F. Sabath, E.L. Mokole (Springer, New York, 2014).

[33] G. Gaborit, P. Jarrige, F. Lecoche, J. Dahdah, E. Duraz, C. Volat, and L. Duvillaret, , IEEE Trans. Plasma Sci. **42**, 1265 (2014).

[34] G. A. Massey, D. C. Erickson, and R. A. Kadlec, Appl. Opt. **14**, 2712 (1975).

[35] L. Gillette, G. Gaborit, C. Volat, J. Dahdah, F. Lecoche, P. Jarrige, and L. Duvillaret, in Proceedings of the IEEE Electrical Insulation Conference (EIC), Philadelphia, June 2014, edited by P. Gaberson, 142.

[36] J.-L Lasserre, P.Bruguière, L. Duvillaret, and G. Gaborit, Chocs – Revue scientifique et technique de la Direction des applications militaires **44**, 85 (2013).

[37] W.-K. Kuo, and D.-T. Tang, Rev. Sci. Instrum. **76,** 055111 (2005).

[38] C. Volat, M. Jabbari, M. Farzaneh, and L. Duvillaret, IEEE Trans. Dielect. El. In. **20**, 194 (2013).

[39] K. Yang, G. David, J.-G. Yook, I. Papapolymerou, L.P.B. Katehi, and J.F. Whitaker, IEEE Trans. Microw. Theory Tech. **48,** 288 (2000).

[40] M. Bernier, L. Duvillaret, G. Gaborit, A. Paupert, and J.-L Lasserre, IEEE Sens. J. **9**, 61 (2008).

[41] Y. Gaeremynck, P. Jarrige, L. Duvillaret, G. Gaborit, and F. Lecoche, PIERS Online **7**, 206 (2011).

[42] Y. Gaeremynck, G. Gaborit, L. Duvillaret, M. Ruaro, and F. Lecoche, Appl. Phys. Lett. **99**, 141102 (2011).

[43] C. Strangio, A. Caruso, Laser Part. Beams **16**, 45 (1998); Inertial fusion progress report (1992-1993), ENEA, RT/ERG/FUS/93/67, 1994;

[44] M. Kobayashi, M. Ishii, K. Harada, and I. Yamaga, Nucl. Instrum. Meth. A **372,** 45 (1996).

[45] H. Shimizu et al, Nucl. Instrum. Meth. A **550**, 258 (2005).

[46] J. Hua, H.J. Kim, G. Rooh, H. Park, S. Kim, and J. Cheon, Nucl. Instrum. Meth. A **648**, 73 (2011).

[47] M. Marinelli et al, Appl. Surf. Sci. **22**, 104 (2013).

[48] D. Margarone et al, Radiat. Eff. Defects Solids **163**, 463 (2008).

[49] R. De Angelis, F. Consoli, C. Verona, G. Di Giorgio, P. Andreoli, G. Cristofari, M. Cipriani, and F. Ingenito, "Time-of-flight and x-ray detectors based on dual-diamond assembly for laser produced plasmas in the ABC facility" to be submitted to J. Instrum.

[50] H.A. Baldis, E.M. Campbell and W.L. Kruer, in *Physics of Laser Plasma*, edited by M.N. Rosenbluth and R.Z. Sagdeev, Handbook of Plasma Physics Vol. 3, (North-Holland, Amsterdam, 1991).

[51] S. Eliezer, *The interaction of high-power lasers with plasmas* (Institute of Physics Publishing, London, 2002).

[52] N.G. Basov, Y.A. Zakharenkov, N.N. Zorev, G.V. Sklizkov, A.A. Rupasov, and A.S. Shikanov, *Heating and compression of thermonuclear targets by laser beams* (Cambridge University Press, Cambridge, 1986).

[53] S. Barbarino, and F. Consoli, IEEE Trans. Antennas Propag. **58,** 4074 (2010).

[54] M. A. Furman, and M.T.F. Pivi, Phys.Rev.ST Accel.Beams **5,** 124404 (2002); Erratum-ibid. **16**, 069901 (2013); SLAC-PUB-9912, LBNL-49771, CBP-NOTE-415 (2002).

[55] J. Cikhardt et al, Rev. Sci. Instrum. **85**, 103507 (2014).